

100

THE RELATIONSHIP BETWEEN THE PERSISTENT WINTER CLOUD
ZONE AND THE JET STREAM IN THE
TROPICAL SOUTHWEST PACIFIC

[Faint, illegible text]

A THESIS SUBMITTED TO THE GRADUATE DIVISION OF THE
UNIVERSITY OF HAWAII IN PARTIAL FULFILLMENT
OF THE REQUIREMENTS FOR THE DEGREE OF

MASTER OF SCIENCE

IN GEOSCIENCES-METEOROLOGY

AUGUST 1971 *Murakami*

C. S. Ramage
Ronald C. Taylor
By

Hayward A. L. Osborn

Thesis Committee:

Takio Murakami, Chairman
Colin S. Ramage
Ronald C. Taylor

We certify that we have read this thesis and
that in our opinion it is satisfactory in scope
and quality as a thesis for the degree of Master
of Science in Geosciences-Meteorology.

THESIS COMMITTEE

Takio Murakami

Chairman

C. S. Ramage

Ronald C. Taylor

ABSTRACT

The strength of the sub-tropical jet stream in the southwest Pacific has been rather a mystery. By performing a scale-analysis of the equations of motion simplified equations for synoptic scale motions in the tropics are derived. This allows the determination of vertical velocity, and thus a study of the kinetic energy processes can be made. For the case considered it is found that there is kinetic energy generation within a cloud zone to the north of the jet stream. This energy is transported aloft and southwards towards the jet stream. It is suggested that such a process is partially responsible for the maintenance of the jet stream.

TABLE OF CONTENTS

ABSTRACT ii

TABLE OF CONTENTS iii

LIST OF FIGURES iv

I. INTRODUCTION 1

II. BASIC EQUATIONS 3

III. SCALE ANALYSIS 5

IV. DISCUSSION OF EQUATIONS 11

V. THE SITUATION OF 20TH JUNE, 1963 12

VI. COMPUTATIONAL DETAILS AND RESULTS 16

VII. KINETIC ENERGY 28

VIII. CONCLUSIONS 40

ACKNOWLEDGEMENT 42

REFERENCES 43

12. Kinetic Energy of the Solar Wind 78

13. Kinetic Energy of the Solar Wind 81

14. Kinetic Energy of the Solar Wind 83

15. Kinetic Energy of the Solar Wind 85

16. Kinetic Energy of the Solar Wind 87

17. Kinetic Energy of the Solar Wind 89

18. Kinetic Energy of the Solar Wind 91

LIST OF FIGURES

1.	Surface Analysis 0000GMT 20th June, 1963	13
2.	850mb Analysis 0000GMT 20th June, 1963	14
3.	300mb Analysis 0000GMT 20th June, 1963	15
4.	Computed Geopotential Heights 850mb	17
5.	Observed Geopotential Heights 850mb	18
6.	Computed Geopotential Heights 300mb	19
7.	Observed Geopotential Heights 300mb	20
8.	Vertical Motion 775mb	23
9.	Vertical Motion 600mb	24
10.	Vertical Motion 400mb	25
11.	Vertical Motion 200mb	26
12.	The Generation Term 775mb	30
13.	Vertical Transport of Kinetic Energy 775mb	31
14.	Kinetic Energy Flux Across the Boundary 400mb	32
15.	Potential Energy Flux Across the Boundary 400mb	33
16.	Kinetic Energy Flux Across the Boundary 200mb	35
17.	Potential Energy Flux Across the Boundary 200mb	36
18.	Energy Processes of the Area Equator - 20S, 120E - 170E ...	37

I. INTRODUCTION

During winter the zone of maximum cloudiness - the "convergence zone" - in the tropical Southwest Pacific is oriented, in the mean, roughly northwest-southeast from New Guinea to near Fiji (Sadler, 1969). On many occasions this zone is marked mainly by extensive altostratus with some high cloud, and, as it does not fit into ordinary ideas of convergence zones, it will be referred to here as the cloud zone.

By the use of isentropic analyses Hill (1963) has shown that the vertical motion in the cloud zone is initiated by a trough and jet stream in the upper tropospheric westerlies. Campbell (1968) also showed that much of the rainfall over eastern Australia is related to an upper trough. This trough in the eastern Australian region is a familiar feature on upper level charts in winter (Ramage, 1970). The associated sub-tropical jet is extremely strong and reaches speeds of over 200 knots at times. This jet is more or less anchored (Muffatti, 1963).

The strength of the jet stream is rather a mystery. It may be compared with the winter jet stream over eastern Asia and Japan. The strength of this jet can be accounted for largely by the Himalayan - Tibetan mountains (Ramage, 1960). Australia does not have comparable mountains so a similar explanation can not be used. Neither are there large land-sea temperature contrasts. The problem is tackled here from the kinetic energy point of view. Hill (1963) has shown that, for the situations he studied, there is ascending motion towards the jet stream from the area of the cloud zone. It therefore seems possible that kinetic energy

generated within the cloud zone would be transported aloft to help maintain the jet stream. This possibility is examined here for a particular situation, the 20th June, 1963.

The vertical motion field is required for this discussion and its determination is most important. It is known that use of the continuity equation produces large errors at the higher levels. It is therefore necessary to take a different approach. Scale analyses (Charney and Eliassen, 1949, Phillips, 1962) have been used in middle latitudes to produce prognostic systems. These systems have included an ω -equation, but are applicable only where Rossby Numbers are less than one. In the tropics Rossby Numbers can be of order one or more so the same equations can not be used.

A scale analysis which applies to the tropical area and to synoptic systems can be made. This allows the determination of the pressure field from the wind field and finally leads to the vertical motion field. This was done by using a five level model. The results were then used to discuss the kinetic energy processes within the vicinity of the cloud zone and jet stream.

On the 20th June, 1963 the jet stream east of Australia was very strong with a maximum of more than 180 knots and the cloud zone was in a more or less normal position. Computations for this situation agree with the suggestion that kinetic energy generated within the cloud zone is transported aloft to help maintain the jet stream.

II. BASIC EQUATIONS

The x, y, p co-ordinate system was used with the following four equations:

The horizontal equations of motion on a tangential plane

$$\frac{\partial u}{\partial t} + u \frac{\partial u}{\partial x} + v \frac{\partial u}{\partial y} + \omega \frac{\partial u}{\partial p} - f v = - \frac{\partial \phi}{\partial x} \quad 1.$$

$$\frac{\partial v}{\partial t} + u \frac{\partial v}{\partial x} + v \frac{\partial v}{\partial y} + \omega \frac{\partial v}{\partial p} + f u = - \frac{\partial \phi}{\partial y} \quad 2.$$

where friction has been ignored. The model deals with the atmosphere above the friction layer so friction is small except near the jet stream where it can be large because of strong vertical and horizontal wind shear (Holopainen, 1963, Kung, 1966). The jet, however, covers only a small area.

The thermal equation

$$\left(\frac{\partial}{\partial t} + u \frac{\partial}{\partial x} + v \frac{\partial}{\partial y} \right) \frac{\partial \phi}{\partial p} + \sigma \omega = 0 \quad 3.$$

assuming no diabatic heating. Where there are no disturbances there is no large scale condensation and heating. However in the situation under consideration the cloud zone covered a broad area and the heating due to condensation could have been important. The cloud zone had been in existence for some days, though, and the heating due to this would have had an effect on the wind and pressure distribution. These quantities are included in the equations and so heating due to condensation is included in this sense. For a more complete discussion the diabatic heating should, of course, be included explicitly.

The equation of continuity

$$\frac{\partial u}{\partial x} + \frac{\partial v}{\partial y} = - \frac{\partial \omega}{\partial p} \quad 4.$$

(III) u = velocity component in the x direction

v = velocity component in the y direction

$w = \frac{dp}{dt}$ = "vertical" velocity component

f = Coriolis parameter

ϕ = geopotential

$\sigma = \frac{\partial \phi}{\partial p} \frac{\partial \ln \theta}{\partial p}$ = a measure of static stability
where θ is the potential temperature.

Riehl (1954) and Palocz (1952) found tropical disturbances (called "easterly waves" by Riehl) with wavelengths of 2000-4000 km and periods of about four days. For the situation on 26th June, 1963 the wavelengths of the disturbances varied from about 2000 km in the lower atmosphere to nearly 10000 km in the upper troposphere. The period of these disturbances was not determined but, from experience, of such situations, 3-5 days would be about average. So a horizontal scale L of 10^6 m can be used and a time scale of 10^5 sec or one day. This can be expressed by L^2/T . Pressure is scaled by the factor $P = 10^2$. This is because we are dealing with the full depth of the atmosphere.

This can be expressed by

$$x = Lx'$$

where x' is non-dimensional and of order 1 or less.

Similarly $y = Ly'$

$$p = Pp'$$

$$u = Uu'$$

$$v = Vu'$$

$$w = \frac{L}{T} w'$$

The vertical velocity factor $\frac{L}{T}$ is used. This is equivalent

III. SCALE ANALYSIS

The basic equations of motion apply to all scales of motion. By applying a scale analysis the basic equations are simplified and the results apply only to the scale of interest, in this case the synoptic scale.

Wind speeds in the tropics are observed to be mainly of the order of 10 m/sec and this value is taken for the wind velocity scale V . Riehl (1954) and Palmer (1952) found tropical disturbances (called "easterly waves" by Riehl) with wavelengths of 2000-4000km and periods of about four days. For the situation on 20th June, 1963 the wavelengths of the disturbances varied from about 2500km in the lower atmosphere to nearly 7000km in the upper troposphere. The period of these disturbances was not determined but, from experience, of such situations, two to five days would be about average. So a horizontal scale L of 10^6 m can be used and a time scale of 10^5 sec or one day. This can be expressed by L/V . Pressure is scaled by the factor $P = 10^3$ mb. This is because we are dealing with the full depth of the atmosphere.

Thus x can be expressed by

$$x = Lx'$$

where x' is non-dimensional and of order 1 or less.

Similarly $y = Ly'$

$$p = Pp'$$

$$u = Vu'$$

$$v = Vv'$$

$$t = \frac{L}{V}t'$$

For vertical velocity the factor $\frac{wP}{L}$ is used. This is equivalent

to 10^{-2} mb sec⁻¹.

Thus $\omega = \frac{VP}{L} \omega'$

The static stability is written $\sigma = \bar{\sigma} \sigma'$

where $\bar{\sigma} = \frac{1}{P} \int_0^P \sigma dp$

Geopotential is expressed by

$$\phi = \bar{\phi} + \phi''$$

where $\bar{\phi}$ is the space-time mean for a particular level and ϕ'' is the departure from this mean. Murakami (1970) has shown that in the

thermal equation the terms $\frac{\partial}{\partial t} \frac{\partial \phi}{\partial p}$ and $\sigma \omega$ balance at all latitudes; $\frac{\partial}{\partial t} \frac{\partial \phi}{\partial p}$ is of the same order as $\sigma \omega$.

Writing this with the scaling factors so far introduced we have:

$$\frac{V}{LP} \frac{\partial}{\partial t'} \frac{\partial \phi''}{\partial p'} \sim \frac{VP}{L} \bar{\sigma} \sigma' \omega'$$

Writing $\phi'' = \tilde{\phi} \phi'$ where $\tilde{\phi}$ contains the dimensions of ϕ'' , and ϕ' is of order 1 or less, we have $\frac{V \tilde{\phi}}{LP} \frac{\partial}{\partial t'} \frac{\partial \phi'}{\partial p'} \sim \frac{VP}{L} \bar{\sigma} \sigma' \omega'$

and by equating the dimensional quantities

$$\frac{V \tilde{\phi}}{LP} \sim \frac{VP \bar{\sigma}}{L} \therefore \tilde{\phi} \sim \bar{\sigma} P^2 = C_g^2$$

where C_g is the phase speed of internal gravity waves.

It is appropriate here to introduce a non-dimensional parameter

$$v = \frac{V}{C_g}$$

v is of order 10^{-1} at all latitudes.

The scaling factor for ϕ'' can now be written

$$\tilde{\phi} = v^{-2} V^2$$

In this analysis ϕ'' was actually expressed by $\phi'' = v^{-2} V^2 \phi$.

This expression yields the geostrophic relation as a first approximation in middle latitudes and eventually gives the quasi-geostrophic

system proposed by Charney and Eliassen (1949). Thus this expression can be used in any latitude.

The Coriolis parameter f is considered as a function of y and is expanded in a Taylor Series.

$$f(y) = f_0 + \frac{2\Omega}{a} \cos \varphi_0 y - \frac{f_0}{a^2} \frac{y^2}{2!} - \frac{2\Omega}{a^3} \cos \varphi_0 \frac{y^3}{3!} + \dots$$

where the subscript indicates a reference latitude and

$$f_0 = 2 \Omega \sin \varphi_0$$

$$\Omega = \text{angular velocity of the earth}$$

$$a = \text{radius of the earth}$$

Equations 1 to 4 are now rewritten in terms of the scaling factors and the non-dimensional quantities. After some cancellation the following system is obtained.

$$\frac{V^2}{L} \left(\frac{\partial u'}{\partial t'} + u' \frac{\partial u'}{\partial x'} + v' \frac{\partial u'}{\partial y'} + \omega' \frac{\partial u'}{\partial p'} \right) - \left(f_0 + 2 \Omega \cos \varphi_0 \frac{L}{a} y' - f_0 \left(\frac{L}{a} \right)^2 \frac{y'^2}{2!} - 2 \Omega \cos \varphi_0 \left(\frac{L}{a} \right)^3 \frac{y'^3}{3!} + \dots \right) V v' = -v' \frac{V^2}{L} \frac{\partial \phi'}{\partial x'} \quad 5.$$

$$\frac{V^2}{L} \left(\frac{\partial v'}{\partial t'} + u' \frac{\partial v'}{\partial x'} + v' \frac{\partial v'}{\partial y'} + \omega' \frac{\partial v'}{\partial p'} \right) + \left(f_0 + 2 \Omega \cos \varphi_0 \frac{L}{a} y' - f_0 \left(\frac{L}{a} \right)^2 \frac{y'^2}{2!} - 2 \Omega \cos \varphi_0 \left(\frac{L}{a} \right)^3 \frac{y'^3}{3!} + \dots \right) V u' = -v' \frac{V^2}{L} \frac{\partial \phi'}{\partial y'} \quad 6.$$

$$v \left(\frac{\partial}{\partial t'} + u' \frac{\partial}{\partial x'} + v' \frac{\partial}{\partial y'} \right) \frac{\partial \phi'}{\partial p'} + \sigma' \omega' = 0 \quad 7.$$

$$\frac{\partial u'}{\partial x'} + \frac{\partial v'}{\partial y'} = - \frac{\partial \omega'}{\partial p'} \quad 8.$$

Now let $\frac{L}{a} = \hat{\beta}$

$\hat{\beta}$ is of order 10^{-1} and non-dimensional.

The Rossby Number ϵ is given by $\epsilon' = \frac{f_0 L}{V}$

and another non-dimensional parameter γ is defined by $\gamma' = \frac{2 \Omega \cos \varphi_0 L}{V}$

If the equator is taken as the reference latitude then

$$\epsilon' = 0$$

and γ^{-1} is of order 10.

In tropical latitudes within 20° of the equator ϵ^{-1} is of order 1 or less and γ^{-1} is of order 10.

The horizontal component equations 5 and 6 can now be written

$$\nu \left(\frac{\partial u'}{\partial x'} + u' \frac{\partial u'}{\partial x'} + v' \frac{\partial u'}{\partial y'} + \omega' \frac{\partial u'}{\partial p'} \right) - \left(\nu \epsilon^{-1} + \nu \gamma^{-1} \beta^2 y' - \nu \epsilon^{-1} \beta^2 \frac{y'^2}{2!} - \nu \gamma^{-1} \beta^3 \frac{y'^3}{3!} + \dots \right) v' = - \frac{\partial \phi'}{\partial x'} \quad 9.$$

$$\nu \left(\frac{\partial v'}{\partial x'} + u' \frac{\partial v'}{\partial x'} + v' \frac{\partial v'}{\partial y'} + \omega' \frac{\partial v'}{\partial p'} \right) + \left(\nu \epsilon^{-1} + \nu \gamma^{-1} \beta^2 y' - \nu \epsilon^{-1} \beta^2 \frac{y'^2}{2!} - \nu \gamma^{-1} \beta^3 \frac{y'^3}{3!} + \dots \right) u' = - \frac{\partial \phi'}{\partial y'} \quad 10.$$

u' , v' , ω' and ϕ' are now expanded in an infinite power series of ν

e.g. $u' = u_0 + \nu u_1 + \nu^2 u_2 + \nu^3 u_3 + \dots$

where u_0 , u_1 , u_2 etc. are of order 1 or less.

As ν is of order 10^{-1} this series converges.

These expressions are substituted into equations 7 to 10. If, then, terms of order ν^0 are picked out the following system is obtained.

$$\frac{\partial \phi_0}{\partial x'} = \frac{\partial \phi_0}{\partial y'} = 0$$

$$\therefore \phi_0 = 0$$

$$\omega_0 = 0$$

$$D_0 = 0$$

11.

where

$$D_0 = \frac{\partial u_0}{\partial x'} + \frac{\partial v_0}{\partial y'}$$

Equations 11 are the first approximations to the equations for synoptic scale motions in the tropics. The pressure gradient is given as zero, in actual fact it is observed to be small.

Similarly for divergence and vertical motion.

Terms of order v^1 give the following set

$$\omega_1 = 0$$

$$D_1 = 0$$

$$\begin{aligned} \frac{\partial u_0}{\partial t'} + u_0 \frac{\partial u_0}{\partial x'} + v_0 \frac{\partial u_0}{\partial y'} - (\varepsilon^{-1} + \gamma^{-1} \hat{\beta} y') v_0 &= - \frac{\partial \phi_1}{\partial x'} \\ \frac{\partial v_0}{\partial t'} + u_0 \frac{\partial v_0}{\partial x'} + v_0 \frac{\partial v_0}{\partial y'} + (\varepsilon^{-1} + \gamma^{-1} \hat{\beta} y') u_0 &= - \frac{\partial \phi_1}{\partial y'} \end{aligned} \quad 12.$$

From the last two equations of 12 vorticity and divergence equations can be obtained. They are

$$\frac{\partial \zeta_0}{\partial t'} + u_0 \frac{\partial \zeta_0}{\partial x'} + v_0 \frac{\partial \zeta_0}{\partial y'} + \gamma^{-1} \hat{\beta} v_0 = 0 \quad 13.$$

where

$$\zeta_0 = \frac{\partial v_0}{\partial x'} - \frac{\partial u_0}{\partial y'}$$

$$2 J(u_0, v_0) - \gamma^{-1} \hat{\beta} u_0 + (\varepsilon^{-1} + \gamma^{-1} \hat{\beta} y') \zeta_0 = \nabla^2 \phi_1 \quad 14.$$

As yet no expression for ω has been found apart from $\omega = 0$.

If we consider terms of order v^2 in the thermal equation we obtain

$$\left(\frac{\partial}{\partial t'} + u_0 \frac{\partial}{\partial x'} + v_0 \frac{\partial}{\partial y'} \right) \frac{\partial \phi_1}{\partial p'} + \sigma' \omega_1 = 0 \quad 15.$$

Returning the dimensions to the v^1 - order equations of continuity, vorticity, and divergence and to the v^2 - order thermal equation we obtain the following:

(i) Continuity equation $\frac{\partial u}{\partial x} + \frac{\partial v}{\partial y} = 0$

(ii) Barotropic vorticity equation $\frac{\partial \zeta}{\partial t} + u \frac{\partial \zeta}{\partial x} + v \frac{\partial \zeta}{\partial y} + \beta v = 0$

(iii) Balance equation $2 J(u, v) - \beta u + f \zeta = \nabla^2 \phi$

(iv) Thermal equation $\left(\frac{\partial}{\partial t} + u \frac{\partial}{\partial x} + v \frac{\partial}{\partial y} \right) \frac{\partial \phi}{\partial p} + \sigma \omega = 0 \quad 16.$

In these equations u has been expressed by

$$u = \nabla u_0$$

Similarly $v = \nabla v_0$

$$f = \frac{v}{L} f_0$$

$$\phi = v^{-1} \nabla^2 (\phi_0 + v \phi_1)$$

$$= \nabla^2 \phi_1 \quad \text{because } \phi_0 = 0$$

$$\omega = \frac{vP}{L} (\omega_0 + v \omega_1 + v^2 \omega_2)$$

$$= \frac{vP}{L} v^2 \omega_2 \quad \text{because } \omega_0 = \omega_1 = 0$$

$\beta = \frac{\partial f}{\partial y}$ the north-south variation of the Coriolis parameter. Where f appears in the balance equation we should have (from the scale analysis) $f_0 + \beta y$ i.e. the β -plane approximation. However substituting f makes little difference and facilitates computation later.

Inventory of NAVAIR 1135

IV. DISCUSSION OF EQUATIONS

Equations 16 are a set of simplified equations for synoptic scale motions in the tropics and form the basis for a diagnostic numerical model.

The fact that divergence is zero implies that the stream function (ψ) field must be given. From this the geopotential field can be obtained by use of the balance equation. Used this way the balance equation is always elliptic and a solution can always be found. Indeed, if used the other way to determine the ψ -field from the ϕ -field, solution becomes impossible near the equator, or unrealistic if modifications are made to the input data (Houghton and Washington, 1969).

It is interesting to note that the complex omega equation used by Krishnamurti (1968) and Baumhefner (1968) is not required.

If a similar scale analysis is applied to middle latitudes, the Rossby Number ϵ is of order 10^{-1} and the quasi-geostrophic scheme (Phillips, 1962) is obtained. The balance equation is found to be the same for middle and tropical latitudes.

V. THE SITUATION OF 20TH JUNE, 1963

On this day surface charts showed the cloud zone of the Southwest Pacific as a broad zone in the New Guinea - Coral Sea area. (Fig.1.) Observations on this day, and also the 19th and 21st, indicated that the zone was composed mainly of altostratus with some high cloud and with only isolated towering cumulus and cumulonimbus.

At the 300mb level a trough lay over eastern Australia and a jet stream maximum of greater than 180 knots lay east of Australia. (Fig.3.)

Streamline-isotach analyses covering the area from 20 N to 50 S and from 100 E to 170 W were made of the levels 850, 700, 500, 300 and 100mb. Data from these analyses were used as input to the numerical model. The levels are not evenly spaced but were chosen according to availability of data. The analyses for the 850mb and 300mb levels are shown in Figs. 2 and 3. Data points (including aircraft and ship observations) are marked by spots.

In some areas the data are rather sparse but, by applying principles of vertical and time continuity and with knowledge of the climatological and synoptic features of the area, very reasonable analyses can be made.



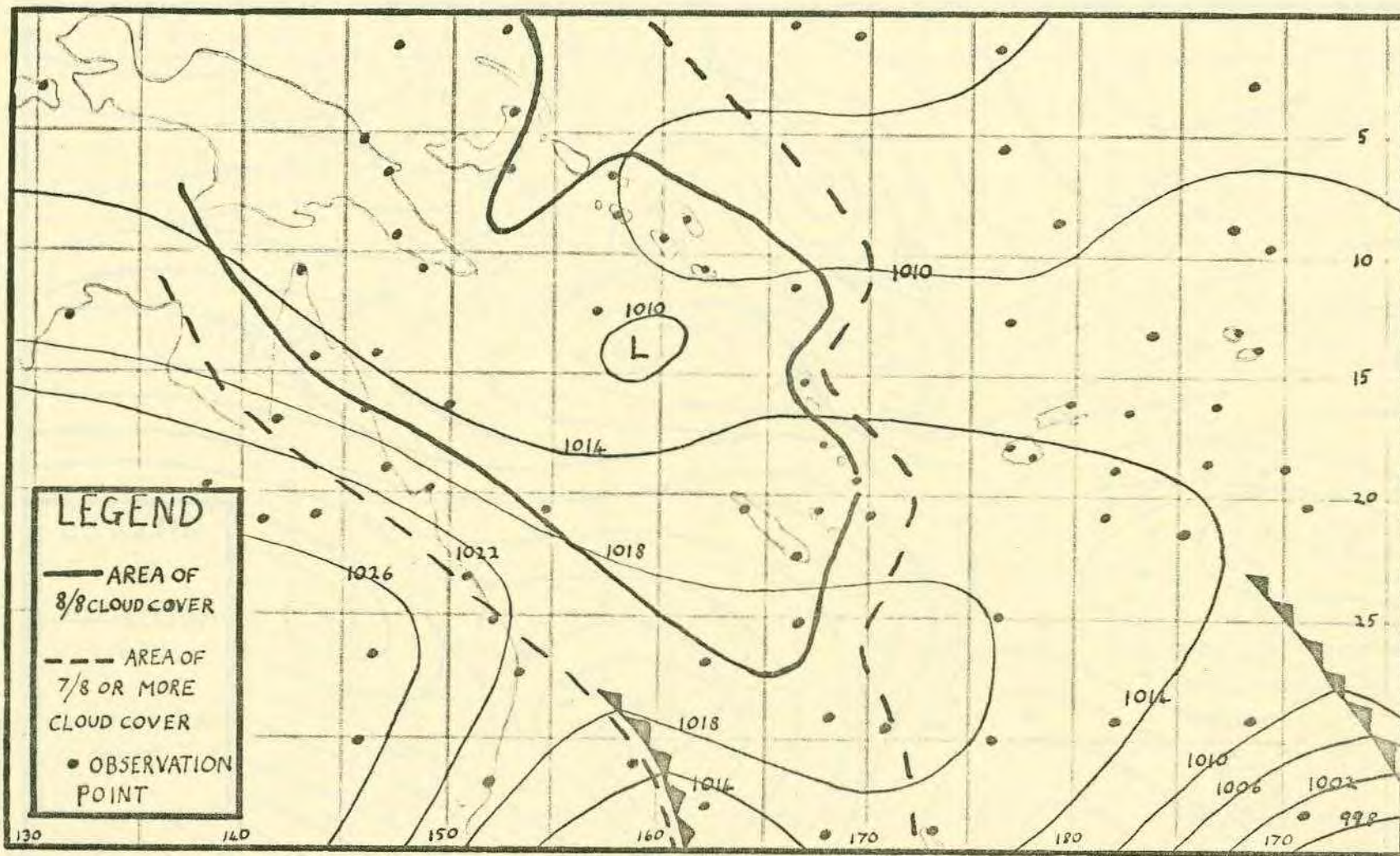


FIGURE 1. Surface Analysis 0000 GMT 20th June, 1963.

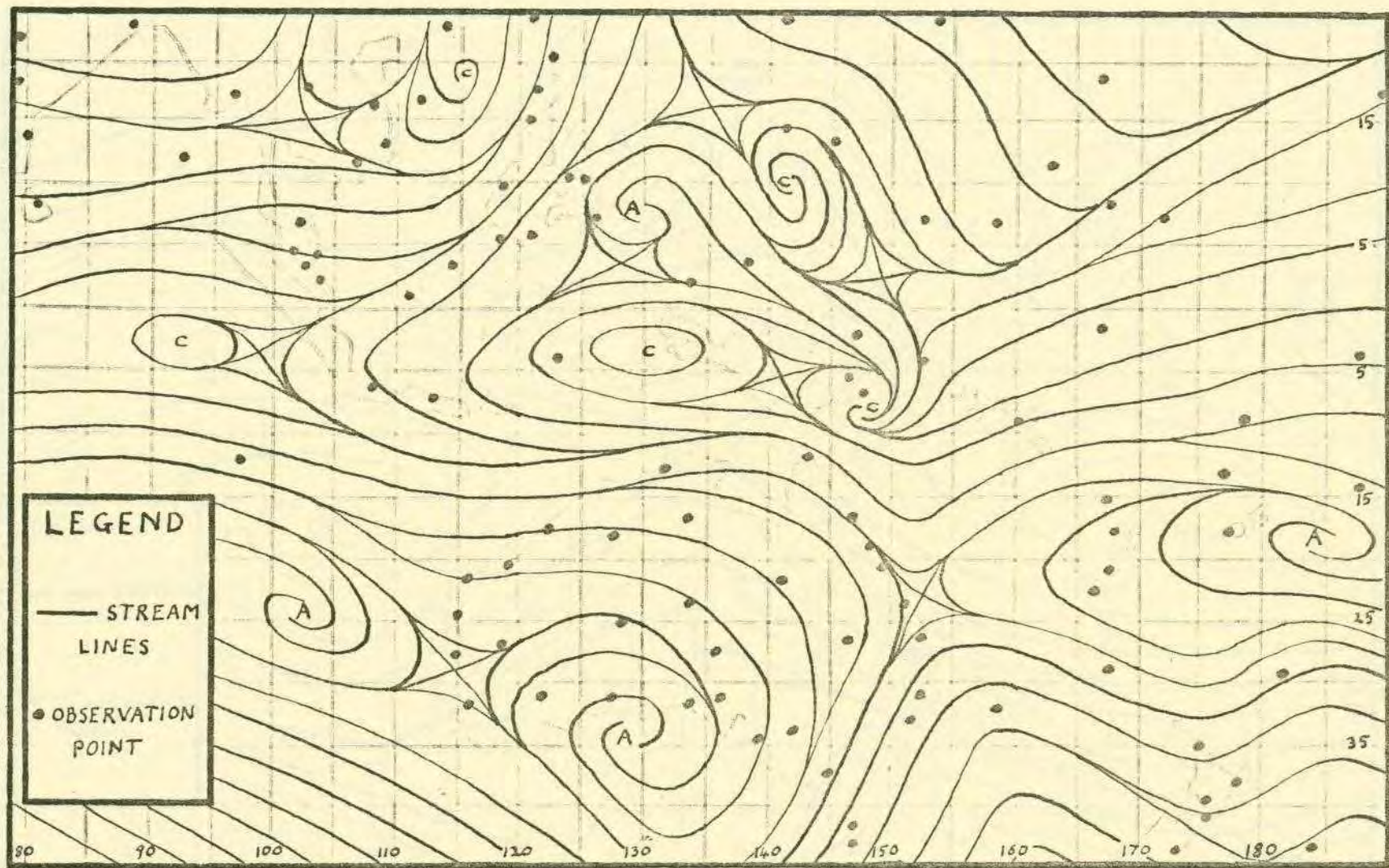


FIGURE 2. 850mb Analysis 0000 GMT 20th June, 1963.

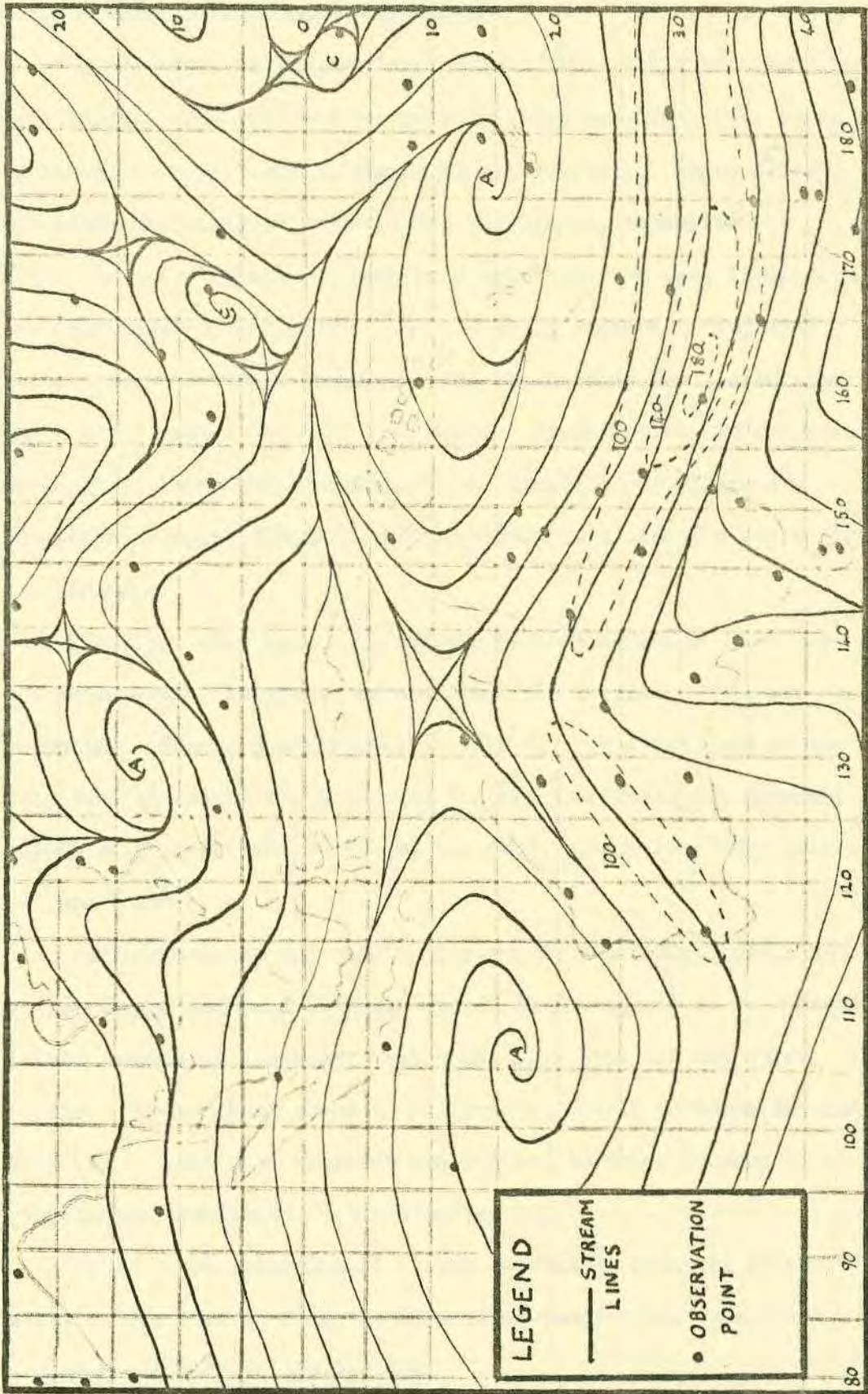


FIGURE 3. 300mb Analysis 0000 GMT 20th June, 1963.

VI. COMPUTATIONAL DETAILS AND RESULTS

As mentioned in the previous section five levels were used for data input. The grid was square with sides measuring five degrees of latitude at the equator (Mercator projection). Where differentiation was required the centered differences technique was used. u and v values for each grid point and for each level were the main input to the model. As the model required divergence to be zero, the stream function field should have been calculated and u and v values obtained from this. To save time, however, and noting that large scale motions of the tropical atmosphere are quasi-nondivergent (Charney, 1963), observed values of u and v were used instead.

The first step was to invert the balance equation to obtain the geopotential height at each of the five levels. This was done using the Liebmann over-relaxation method. Hand-analyses of the geopotential height had been made for all the levels and boundary values of ϕ (required to invert the balance equation) were obtained from these.

For comparison, the results for the 850 and 300mb levels and the corresponding hand analyses are shown in Figs. 4 to 7. There is very reasonable agreement, which was also true for the other levels. When making these comparisons it should be borne in mind that (i) the hand analyses are subject to error because of weak geopotential gradients in the tropics, and,

(ii) the geopotential fields calculated from the balance equation are derived from the streamline-isotach analyses which are more accurate in the tropics.

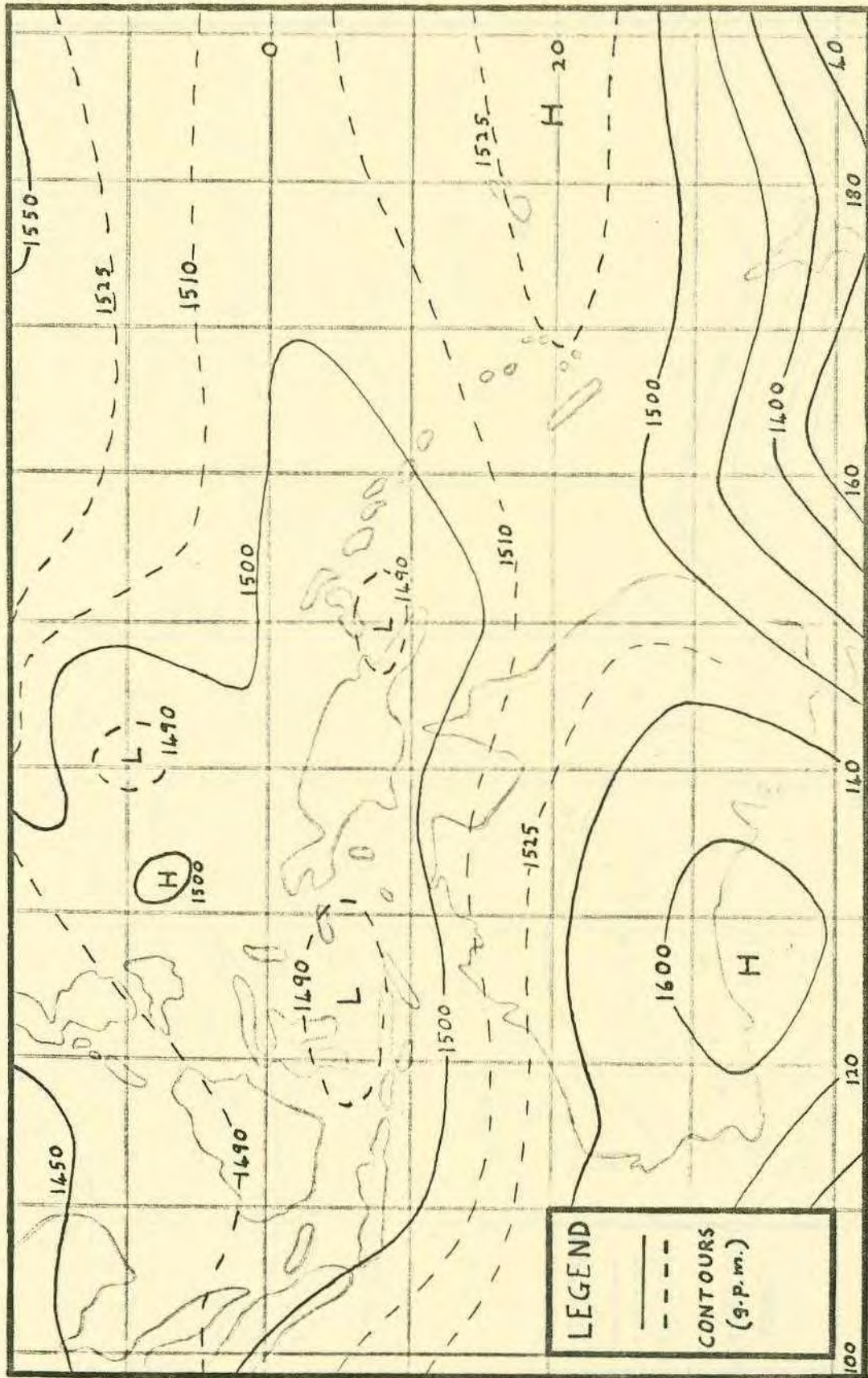


FIGURE 4. Computed Geopotential Heights 850mb.

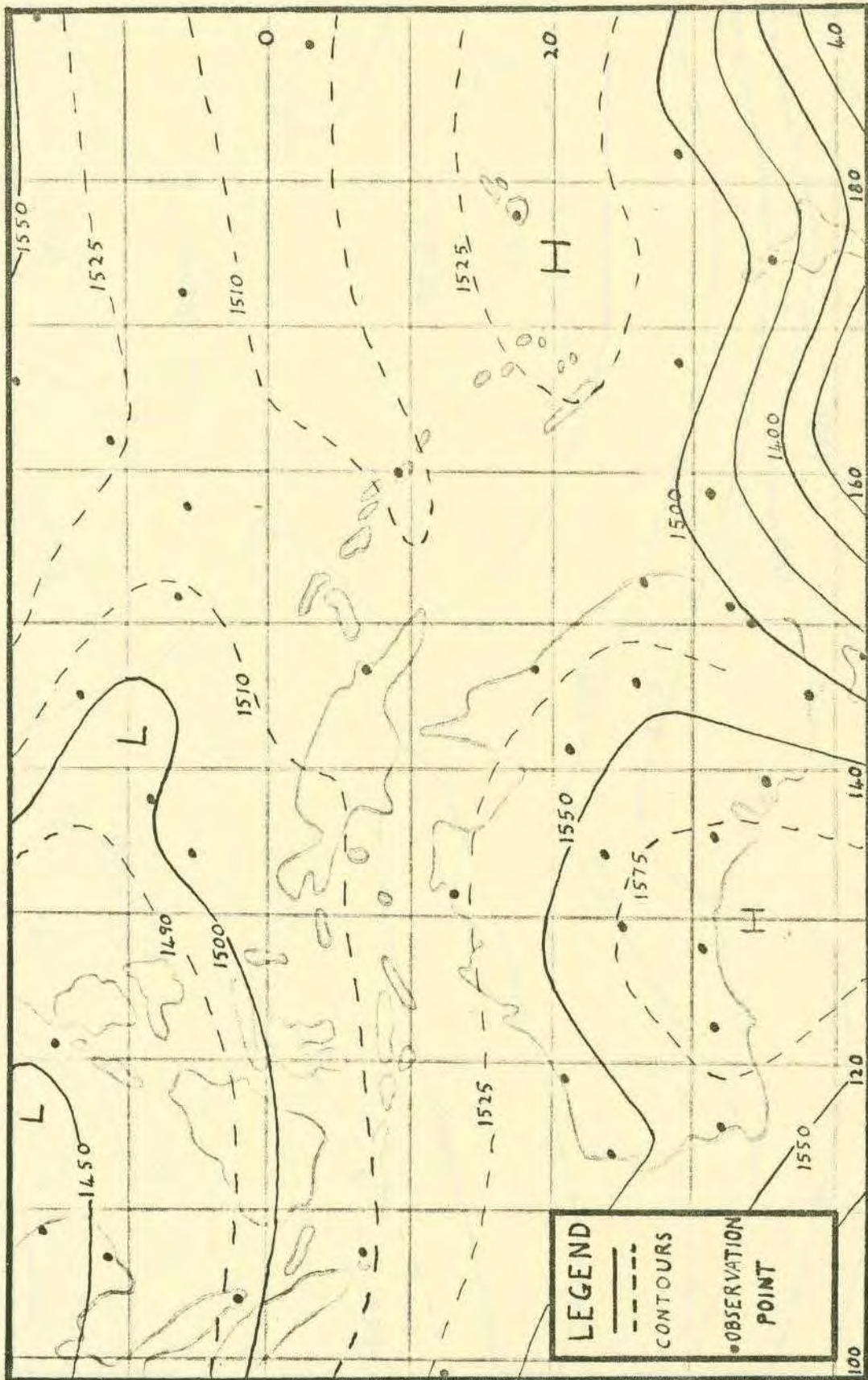


FIGURE 5. Observed Geopotential Heights 850mb

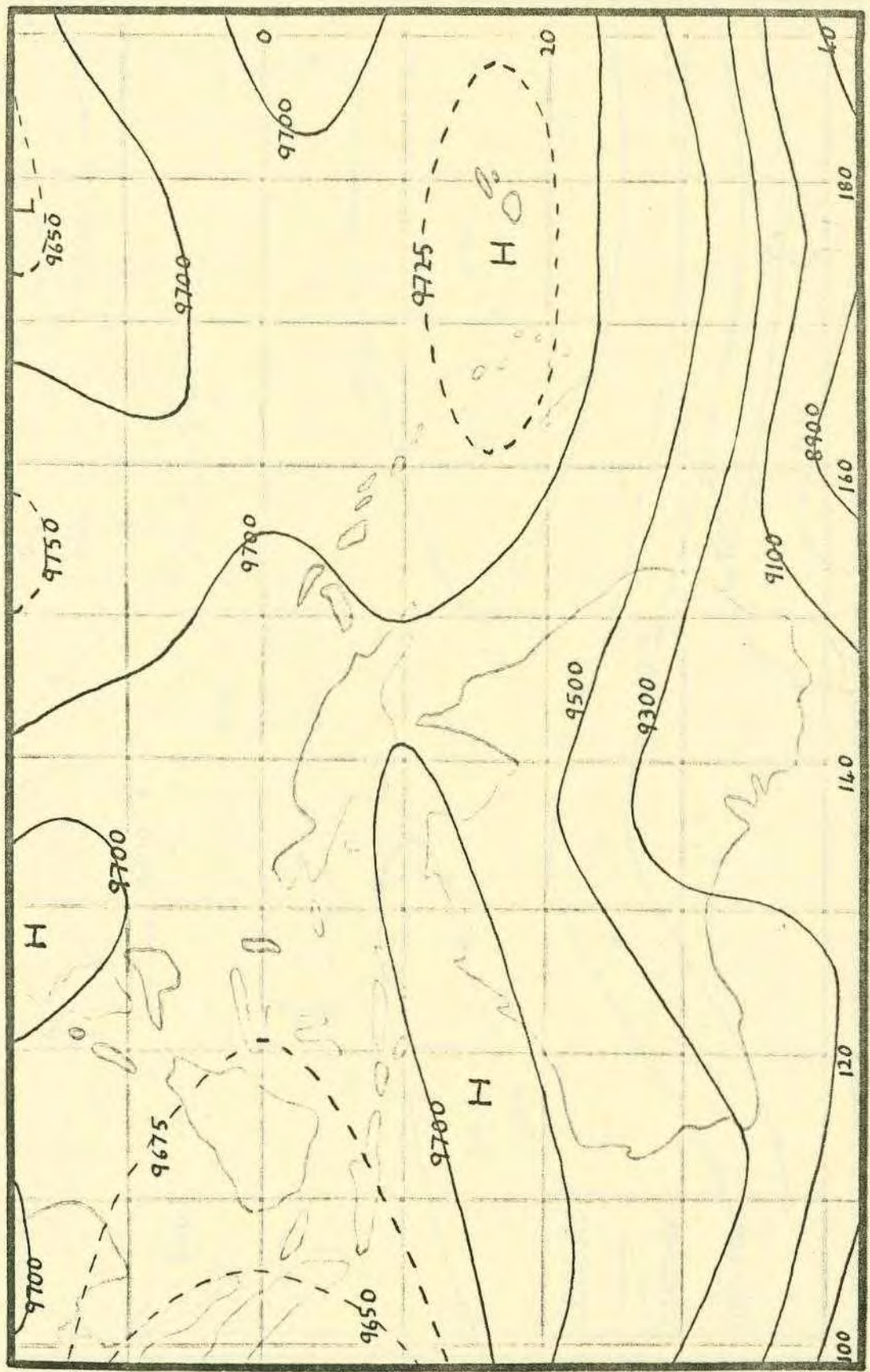


FIGURE 6. Computed Geopotential Heights 300mb.

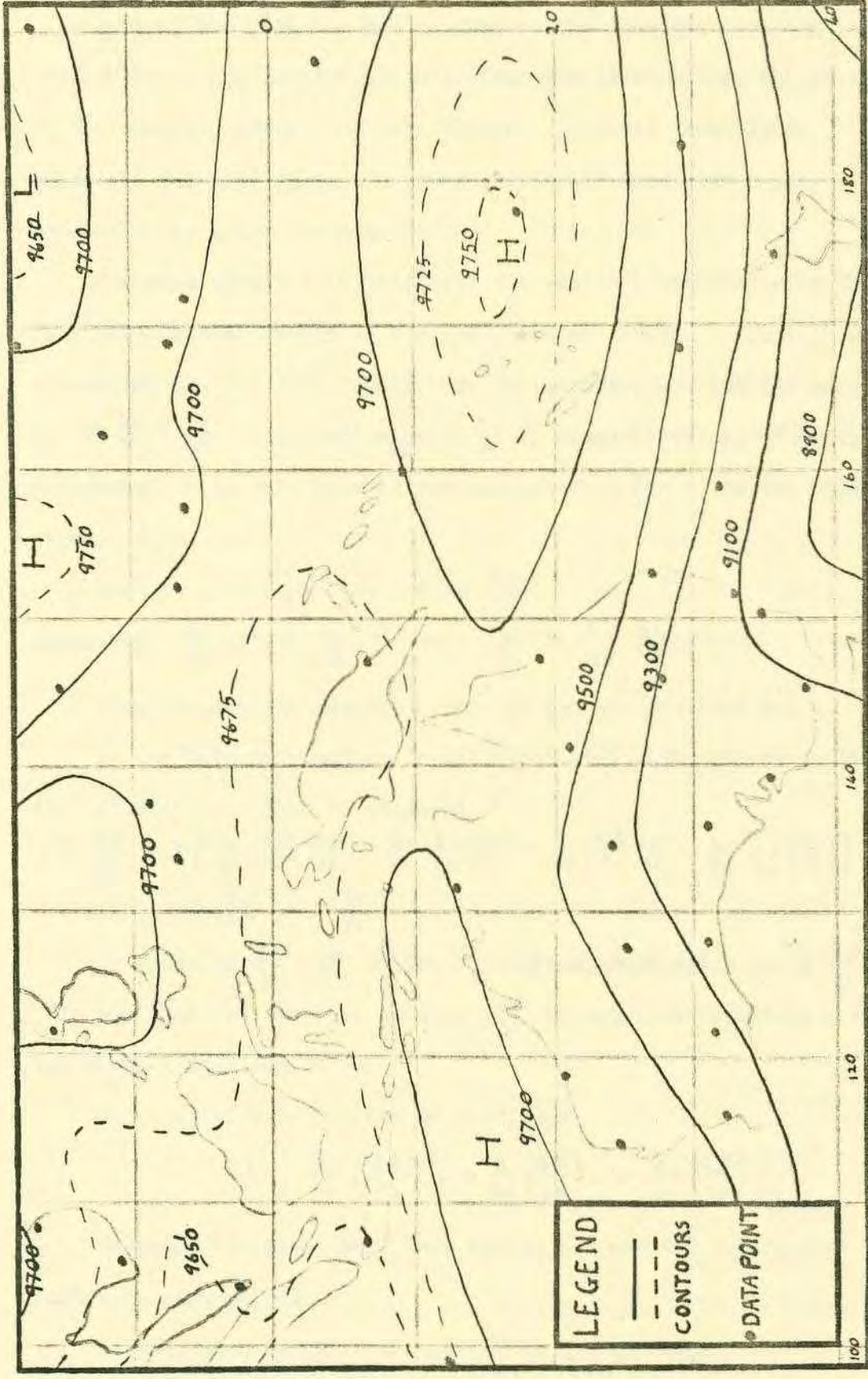


FIGURE 7. Observed Geopotential Heights 300mb.

Some of the high and low centers in the computed geopotential height fields are shifted slightly from the positions of the centers in the analysed height and wind fields. This is probably an effect of the grid size. A finer grid would have given finer resolution of these centers.

The next step was to calculate the vertical velocity ω at the four intermediate levels of 775, 600, 400 and 200mb. First $\frac{\partial \zeta}{\partial t}$ was calculated for the five levels from the barotropic vorticity equation. As $\nabla^2 \frac{\partial \psi}{\partial t} = \frac{\partial \zeta}{\partial t}$, inversion gives $\frac{\partial \psi}{\partial t}$ if boundary values of $\frac{\partial \psi}{\partial t}$ are prescribed. In this case it was assumed that $\frac{\partial \psi}{\partial t} = 0$ on the boundaries.

$$\text{Now } u = -\frac{\partial \psi}{\partial y} \text{ and } v = \frac{\partial \psi}{\partial x}$$

$$\text{Therefore } \frac{\partial u}{\partial t} = -\frac{\partial}{\partial y} \frac{\partial \psi}{\partial t} \text{ and } \frac{\partial v}{\partial t} = \frac{\partial}{\partial x} \frac{\partial \psi}{\partial t}$$

These values are easily calculated and are required below.

If the balance equation is differentiated with respect to time the following equation is obtained

$$\nabla^2 \frac{\partial \phi}{\partial t} = 2 \left[\frac{\partial}{\partial x} \left(\frac{\partial u}{\partial t} \right) \frac{\partial v}{\partial y} + \frac{\partial u}{\partial x} \frac{\partial}{\partial y} \left(\frac{\partial v}{\partial t} \right) - \frac{\partial}{\partial y} \left(\frac{\partial u}{\partial t} \right) \frac{\partial v}{\partial x} - \frac{\partial u}{\partial y} \frac{\partial}{\partial x} \left(\frac{\partial v}{\partial t} \right) \right]$$

$$- \beta \left(\frac{\partial u}{\partial t} \right) + f \frac{\partial \zeta}{\partial t}$$

By assuming $\frac{\partial \phi}{\partial t} = 0$ on the boundaries, relaxation gives $\frac{\partial \phi}{\partial t}$. This was done for the five levels. $\frac{\partial \phi}{\partial t}$ is required to obtain ω from the thermal equation.

The thermal equation can be rewritten

$$\omega = -\frac{1}{\sigma} \left[\frac{\partial}{\partial p} \left(\frac{\partial \phi}{\partial t} \right) + u \frac{\partial}{\partial x} \left(\frac{\partial \phi}{\partial p} \right) + v \frac{\partial}{\partial y} \left(\frac{\partial \phi}{\partial p} \right) \right] \quad 17.$$

Measurements of σ were made and it was decided to use the following mean values.

At the 775mb level $\sigma = .02$ everywhere

At the 600mb level $\sigma = .03$ everywhere
 At the 400mb level $\sigma = .05$ from the equator to 20S
 and $\sigma = .07$ south of 20S
 At the 200mb level $\sigma = .2$ from the equator to 20S
 $\sigma = .3$ from 20 to 29S
 and $\sigma = .4$ south of 29S

Units of σ are $m^2 \text{sec}^{-2} \text{mb}^{-2}$

If u and v are interpolated at the intermediate levels all the terms on the right hand side equation 17 are known and ω can be calculated.

It became apparent that the relaxation process had been affected by the presence of ultra-long waves at the higher levels. Wave number one was filtered out and this produced reasonable results, which are shown in Figs. 8 to 11. The area covered in these figures is smaller than the original area because boundary values are lost each time the centered difference technique is applied.

Of course the results only apply to the tropics, but the calculations have been extended to higher latitudes in the south in order to keep the boundaries sufficiently far away from the area of interest.

If the vertical velocity at 775mb is compared with the 850mb chart, it is found that there is upward motion east of the trough in the Coral Sea - Tasman Sea area and east of the trough northwest of Australia. The maximum of about $10 \times 10^{-4} \text{mb sec}^{-1}$, or about 1 cm/sec, occurs in the central Coral Sea. Subsidence occurs in the anticyclonic area over Australia west of the troughs, and in the easterlies north of the New Hebrides. The vertical

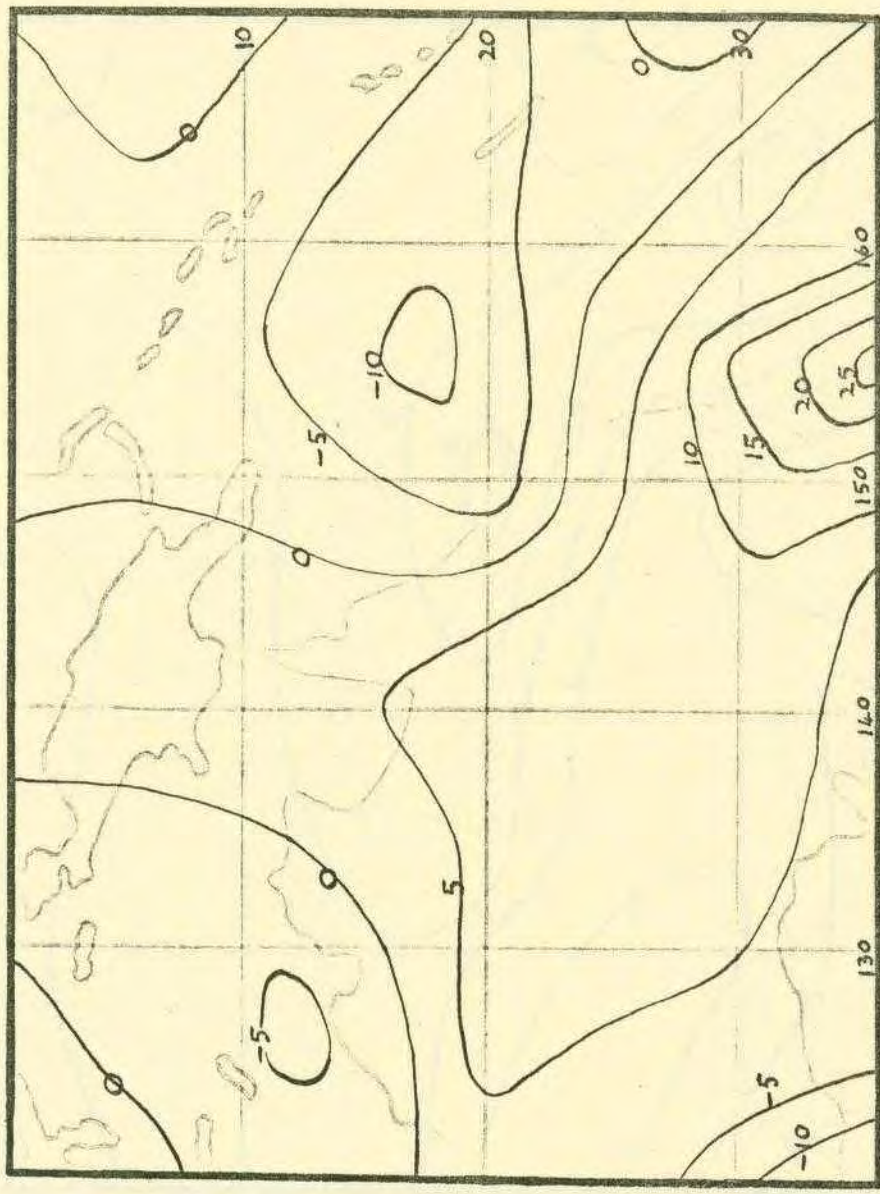


FIGURE 8. Vertical Motion 775mb. Units mb/sec x 10⁻⁴.

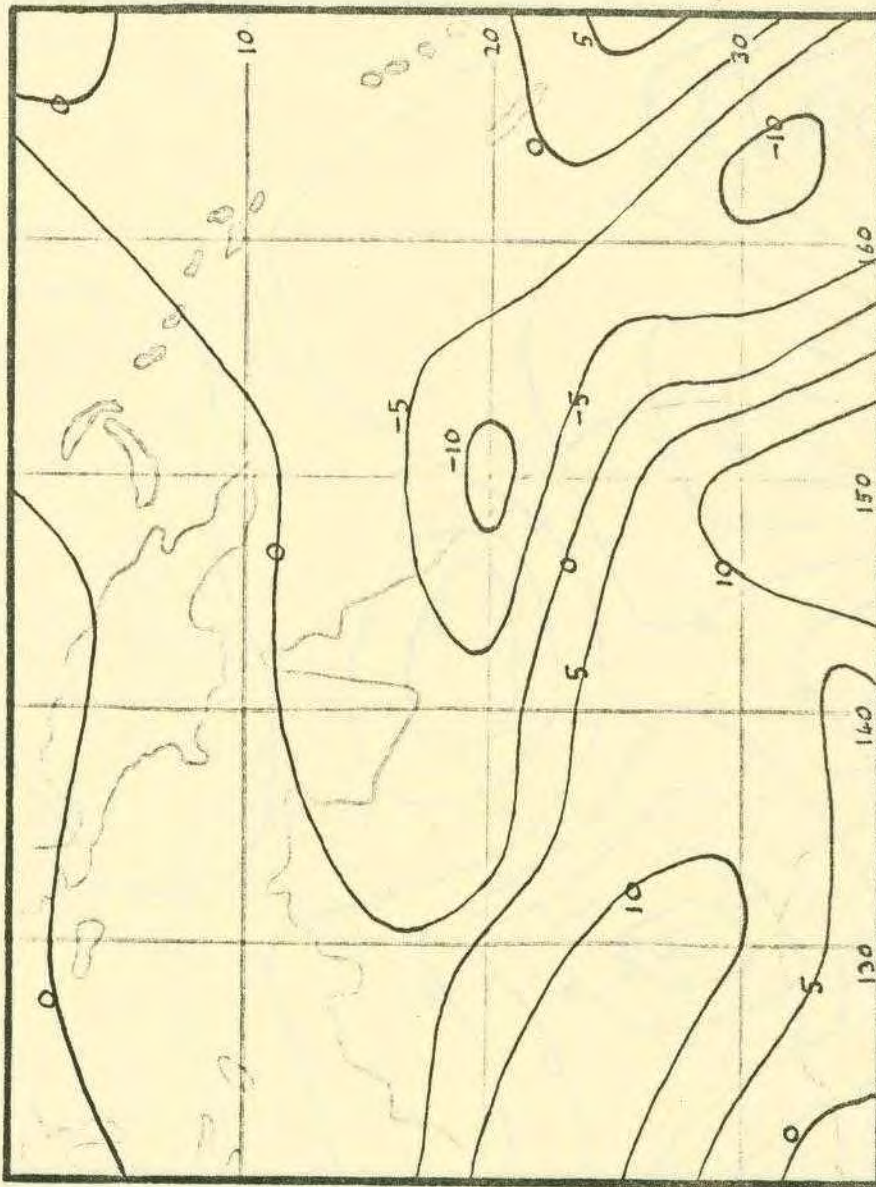


FIGURE 9. Vertical Motion 600mb.

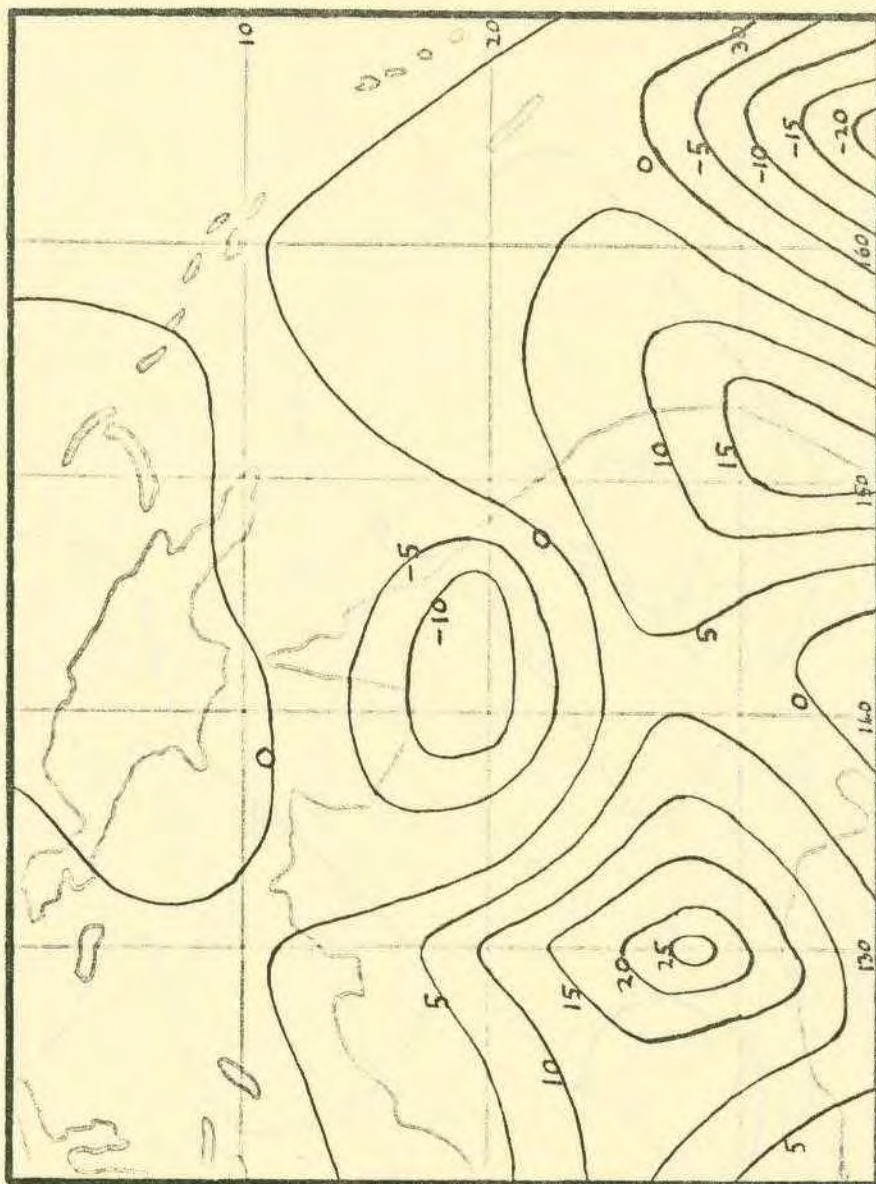


FIGURE 10. Vertical Motion 400mb.

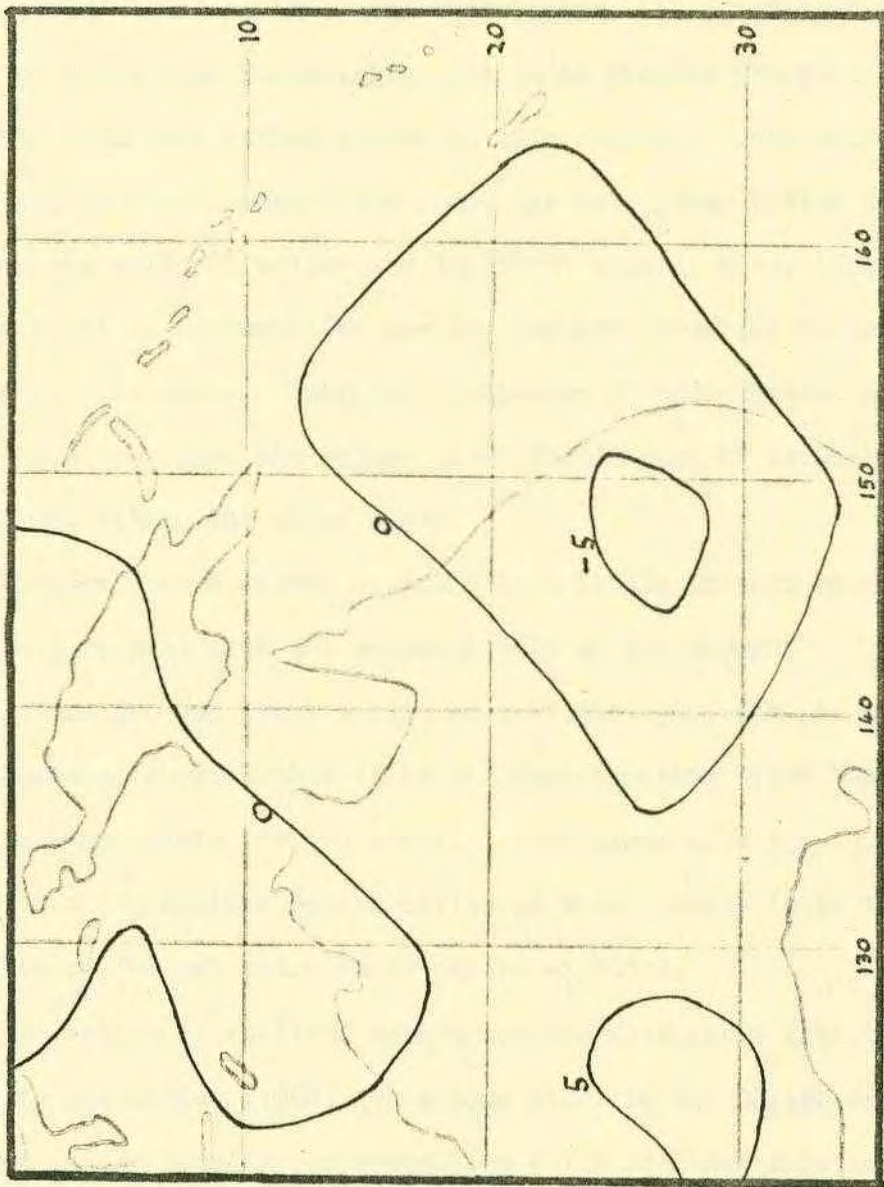


FIGURE 11. Vertical Motion 200mb.

motion field in the Coral Sea area agrees with the cloud distribution shown in Fig. 1, except about New Guinea where this is not true.

The vertical motion at 600mb shows more agreement in this region, but there is a band of weak subsidence running across the cloud zone. Part of this band corresponds with an area of less cloud coverage near Bougainville, but is of greater extent.

The data were rather sparse in this region. More data, resulting in more accurate analyses, may have given better agreement between the vertical motion and the cloud zone. Also, inclusion in the model of condensation heating may have resulted in ascending motion in this area. Certainly inclusion of condensation heating would have increased the values of ω where areas of ascending air were found within the cloud zone.

Maximum upward motion at 600mb is a little further south and west in agreement with the westward tilt of the trough.

At the 400 and 200mb levels most of the cloud zone is overlaid by subsidence showing that it is the upward motion below these levels that is responsible for the cloud. Comparison with the 300mb chart shows that the maximum upward motion at these levels is in the vicinity of the jet entrance as may be expected.

The values of vertical motion compare favourable with those found by Baumhefner (1968) for a case study in the Caribbean. Here he used a more complex omega-equation which included friction and condensation heating.

VII. KINETIC ENERGY

Following Murakami (1959) and Smagorinsky et alia (1965), kinetic energy processes can be treated in the following manner.

From the primitive equations of motion a kinetic energy equation can be obtained.

$$\frac{\partial K}{\partial t} + \underline{V} \cdot \nabla K + \omega \frac{\partial K}{\partial p} = -\underline{V} \cdot \nabla \phi + \underline{V} \cdot \underline{F} \quad 18.$$

where $K = \frac{1}{2}(u^2 + v^2)$

\underline{F} is the frictional force, \underline{V} the horizontal wind, and

∇ is the horizontal operator.

To consider the contribution of a region to the entire atmosphere, equation 18 can be integrated over an area S giving

$$\begin{aligned} \iint_S \frac{\partial K}{\partial t} dS &= -\oint_C V_n (K + \phi') dC - \iint_S \frac{\partial \omega (K + \phi')}{\partial p} dS \\ &+ \iint_S \omega \frac{\partial \phi'}{\partial p} dS + \iint_S \underline{V} \cdot \underline{F} dS \end{aligned} \quad 19.$$

where V_n is the outward normal component of velocity along the boundary C , and ϕ' is the departure from the space mean of ϕ .

The first term on the right contains the flux of kinetic and potential energy across the boundary of the area. The second term is the vertical transport of kinetic and potential energy. The third term is a generation term. It may be written $-\iint_S \omega \alpha' dS$ where α' is the departure from the mean specific volume. The last term is the frictional dissipation of kinetic energy.

Except for the friction term all terms on the right of equation 19 were evaluated for the 20th June, 1963 by using results from the diagnostic model. The region covered was from 120 to 170 degrees East and from the Equator to 20 degrees South. This area is mainly

outside the jet stream and the levels considered are below the tropopause and above the friction layer. Thus friction will be small (Holopainen, 1963, Kung, 1966, Trout and Panofsky, 1969).

As well as performing the integrations, grid point or boundary values of $V_n K$, $V_n \phi'$, ωK , $\omega \phi'$, and $\omega \frac{\partial \phi'}{\partial p}$ were calculated at the 775, 600, 400 and 200mb levels. Integrals of $\frac{\partial \omega K}{\partial p}$ and $\frac{\partial \omega \phi'}{\partial p}$ were naturally calculated at the intermediate levels.

At the 775mb level local boundary values of $V_n K$ and $V_n \phi'$ were small. The generation term $\omega \frac{\partial \phi'}{\partial p}$ shows a maximum within the cloud zone and east of the 850mb trough (Fig.12). This is an area of ascending warm air which releases kinetic energy, as pointed out by Margules. There is a second maximum in the southwest corner where there is subsiding cold air in the anticyclonic region. Maximum vertical transport (ωK) occurs in the same regions (Fig.13) while $\omega \phi'$ is a maximum in the southeastern corner near New Caledonia. This is an area of ascending motion with high values of geopotential.

At the 600mb level $\omega \frac{\partial \phi'}{\partial p}$ is much smaller everywhere but there are still weak maxima in the same areas. $\omega \phi'$ is a maximum in the same area of the cloud zone and ωK is a maximum just southwest of this. Again local boundary values of $V_n K$ and $V_n \phi'$ are relatively small.

At the 400mb level values $\omega \frac{\partial \phi'}{\partial p}$ are small in the area of interest showing that generation of kinetic energy is not important at this level. Maximum upward transport of K and ϕ' is now further west in the region of maximum upward motion (Fig.10). Some local values of $V_n K$ and $V_n \phi'$ are now becoming large and these are shown in figures 14 and 15. There is significant import of both quantities in the southwest corner of the area near a second

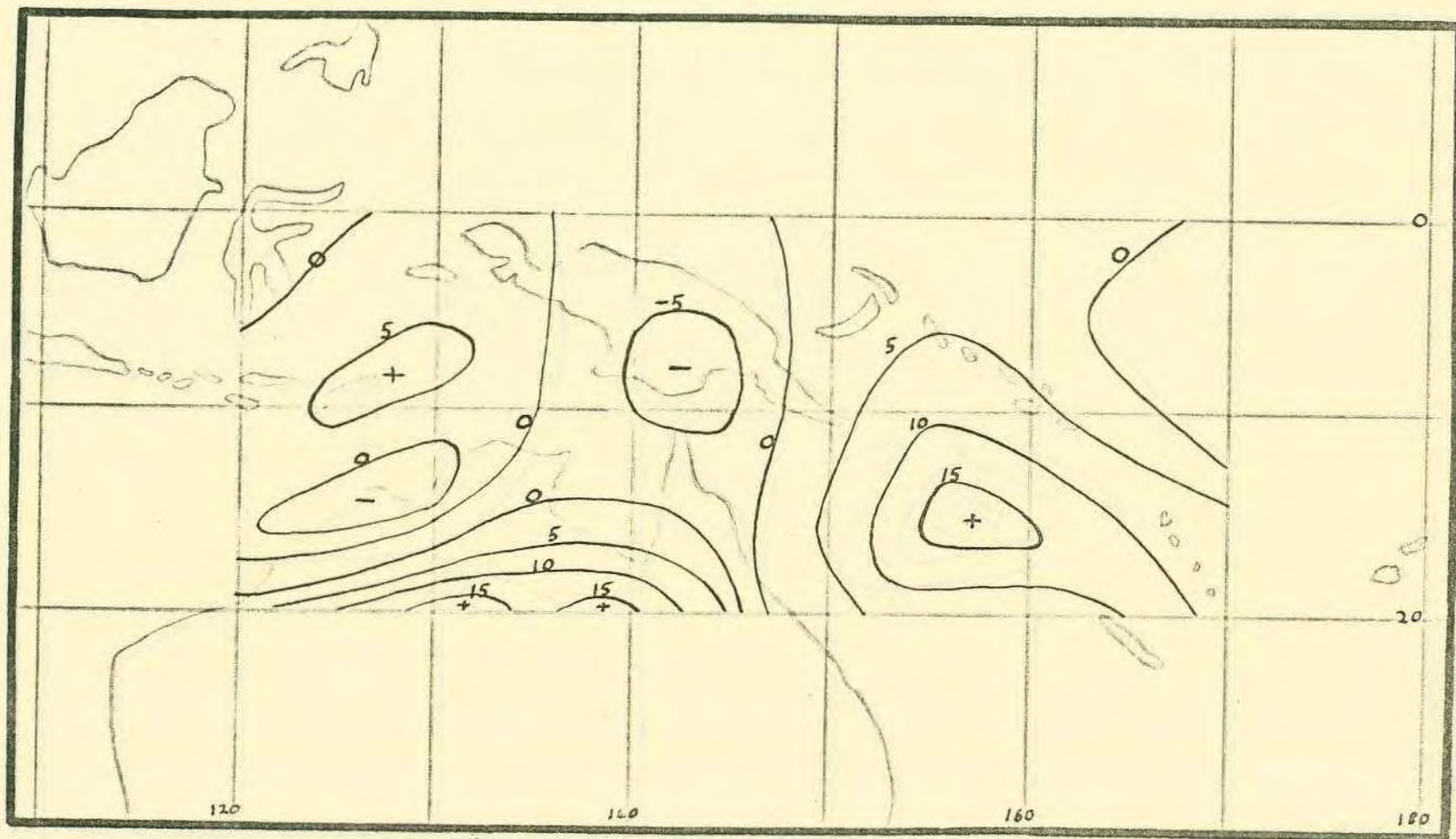


FIGURE 12. The Generation Term 775mb. Units $\text{erg gm}^{-1} \text{sec}^{-1}$.

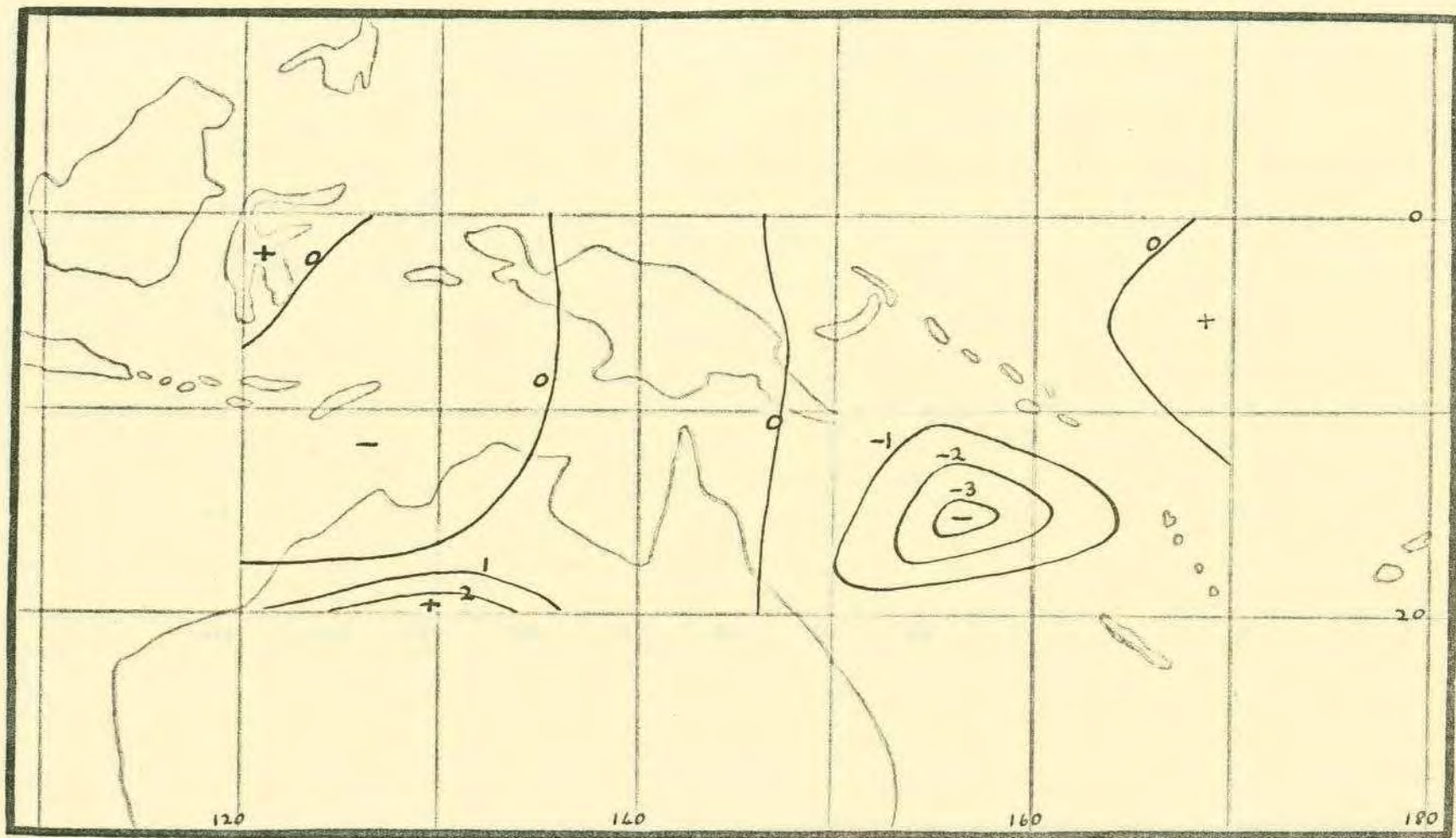


FIGURE 13. Vertical Transport of Kinetic Energy 775mb. Units $\text{erg mb gm}^{-1} \text{sec}^{-1} \times 10^2$.

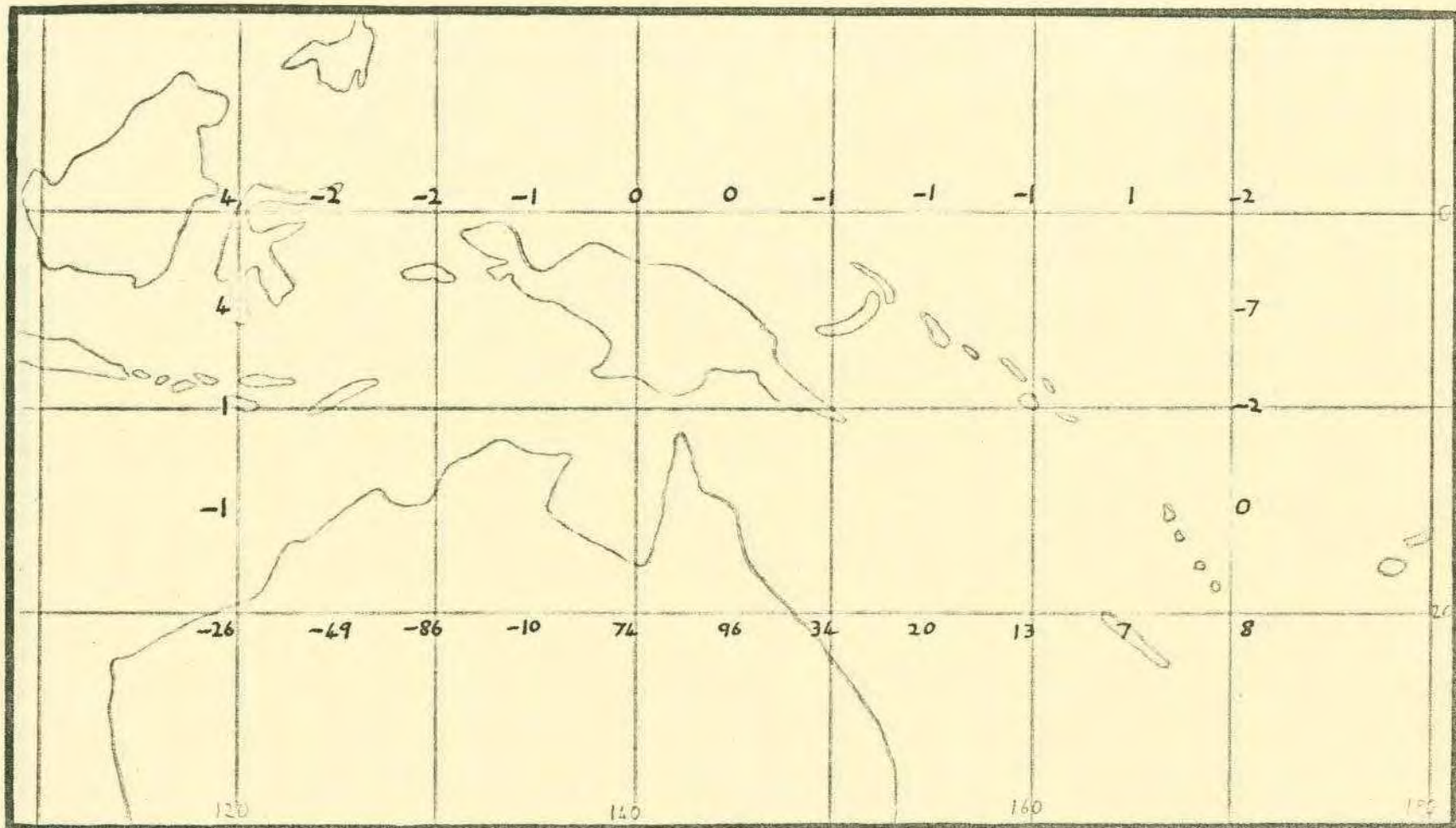


FIGURE 14. Kinetic Energy Flux Across the Boundary 400mb.
 Negative Values Indicate Transport into the Region.
 Units $\text{erg cm}^{-1} \text{sec}^{-1} \times 10^8$.

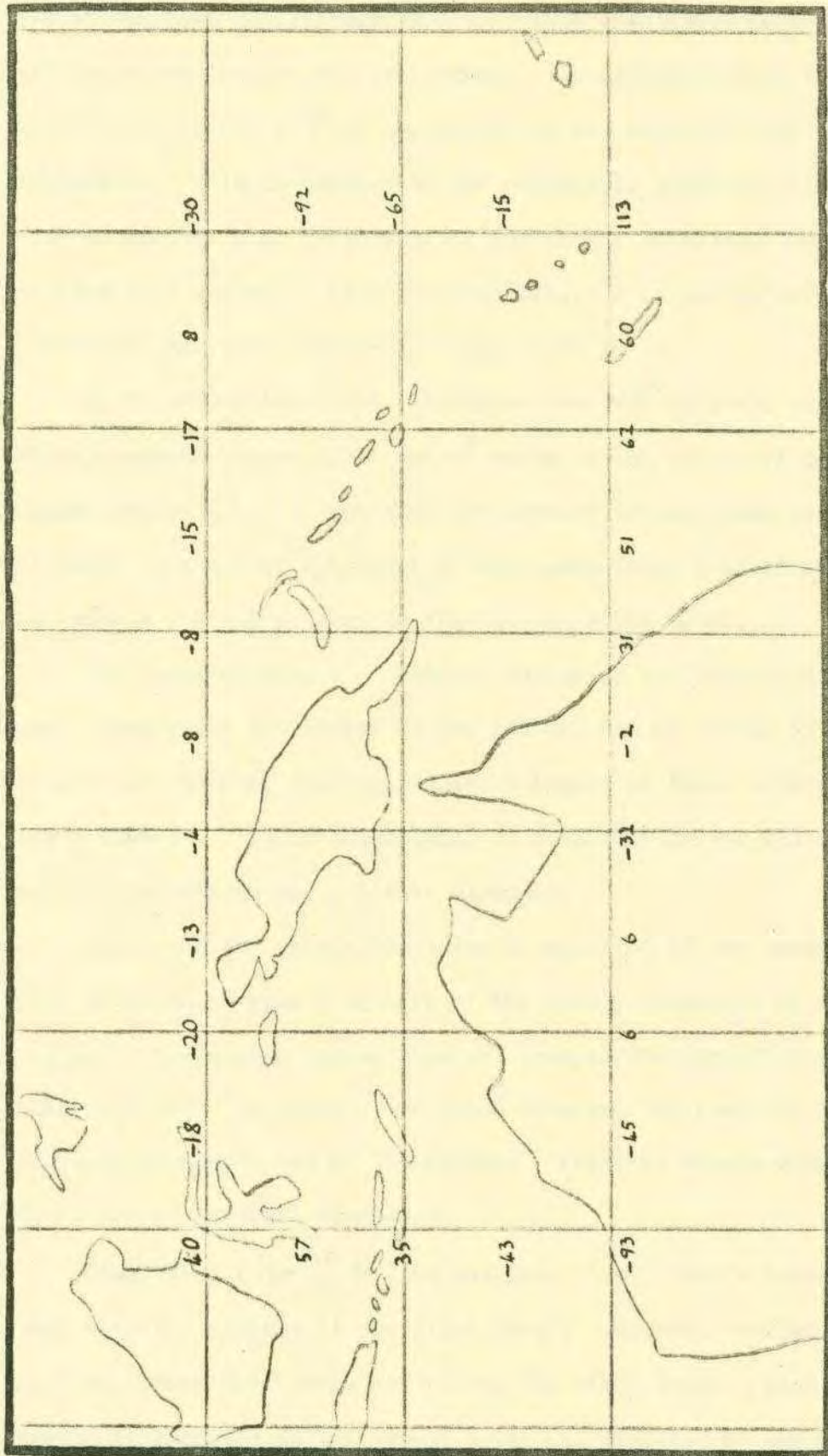


FIGURE 15. Potential Energy Flux Across the Boundary 400mb.

jet stream, and significant export of both quantities in the south and southeast towards the jet stream. In addition there is significant import of ϕ' in the northeast and export in the northwest. This is because in the northeast, there is inflow from an area of high geopotential, and in the northwest there is outflow in a region of high geopotential. This can be seen from a study of the 300mb charts in Figs. 3 and 7.

At the 200mb level the generation term $\omega \frac{\partial \phi'}{\partial p}$ is small everywhere. Maximum upward values of ωk and $\omega \phi'$ occur in the region of maximum upward motion (Fig. 11) and similar downward values occur just west of this. Values of $V_n k$ and $V_n \phi'$ are again large (Fig. 16 and 17) and show a similar pattern to that at the 400mb level.

The combined export of kinetic energy in the south and southeast towards the jet stream at the 400 and 200 mb levels is about 19 per cent greater than the combined import at these levels from the southwest. It is interesting to note that on the following day the jet stream was a little stronger.

Values of the integrated terms of equation 19 are shown in Fig. 18 which is also a summary of the energy processes of the region. Horizontal arrows directed towards the center indicate transport into the region, and those directed out from the center indicate transport out of the region. Vertical arrows show the direction of vertical transport.

Generation ($\iint \omega \frac{\partial \phi'}{\partial p} dS$) is positive at all levels except the top, with the maximum at the 775mb level. As seen earlier, the maximum within this level was within the cloud zone. Kinetic energy is imported at the lowest level and exported at the remaining

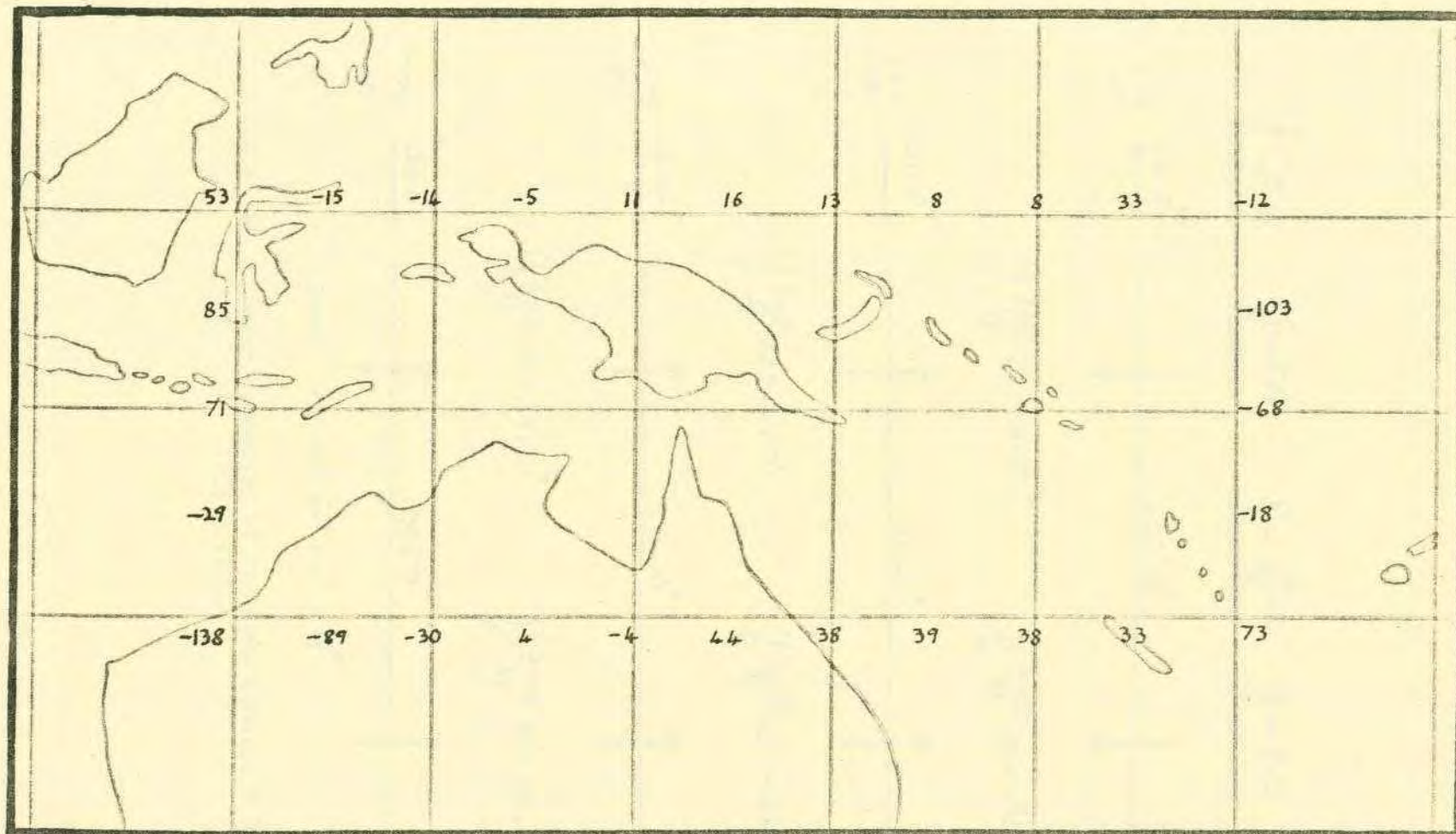


FIGURE 17. Potential Energy Flux Across the Boundary 200mb.

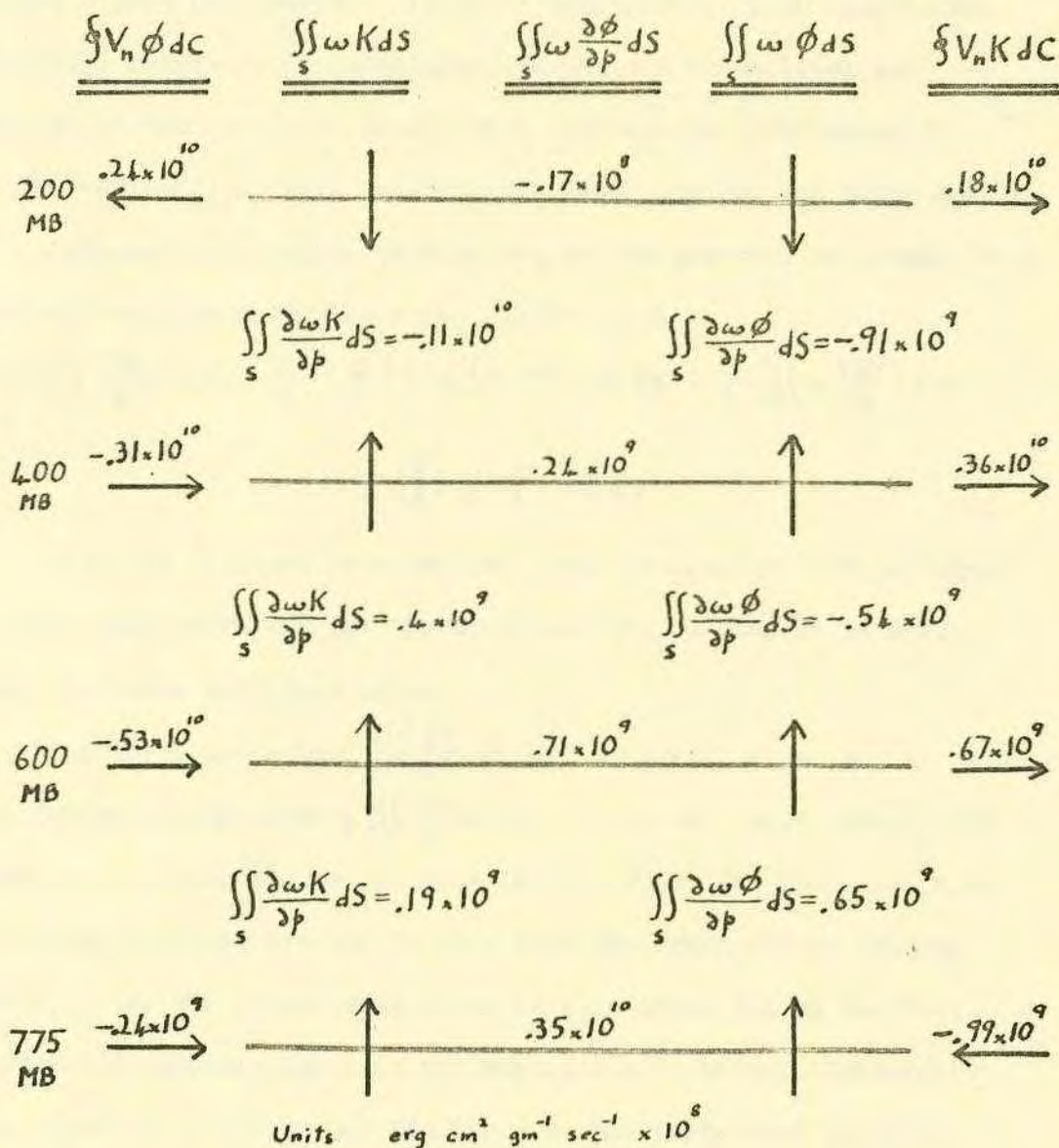


FIGURE 18. Energy Processes of the Area Equator - 20S,
120E - 170E.

levels, the largest values being at the 400 and 200mb levels. Potential energy, however, is imported into the lower three levels and exported at the top, with significant values at all levels except the lowest. Vertical transport of both kinetic and potential energy is directed downwards at the 200mb level and upwards at the remaining levels with convergence (with respect to the vertical) of both quantities between the 200 and 400mb levels.

Integrating equation 19 with respect to pressure we obtain the complete kinetic energy equation for the region.

$$\frac{1}{g} \iiint \frac{\partial K}{\partial t} dS dp = -\frac{1}{g} \iint V_n (K + \phi') dC dp + \frac{1}{g} \iiint \omega \frac{\partial \phi'}{\partial p} dS dp + \frac{1}{g} \iiint \underline{V} \cdot \underline{F} dS dp \quad 20.$$

With the friction term omitted, this integration was performed for the area above and for the area from the equator to 33 South which includes the first area.

$$\text{For the first area } \frac{1}{g} \iiint \frac{\partial K}{\partial t} dS dp = +.11 \times 10^{21} \text{ ergs. sec}^{-1} \quad 21.$$

$$\text{and for the second area } \frac{1}{g} \iiint \frac{\partial K}{\partial t} dS dp = -.12 \times 10^{22} \text{ ergs. sec}^{-1} \quad 22.$$

There is an error due to friction in the result for the first area but as wind speeds are low in this area the error may be assumed small. For the second area there is some error due to the fact that the diagnostic model is not applicable in higher latitudes. This error is probably not too large as the calculated vertical velocities appeared reasonable. Errors due to neglecting the friction term may, however, be large in the vicinity of the jet stream, but they would act to keep the result negative. So, for the whole area, there is a net decrease of kinetic energy. For the first area - the tropical sub-area - there is a net increase of kinetic

energy which makes a positive contribution to the whole area.

It seems that the tropical areas, and in particular the Indian Ocean, may be a source of energy for the sub-tropical jet stream. Results from the previous section suggest a possible model of (i) kinetic energy generation within the cloud zone (ii) transport aloft to the upper troposphere, and then (iii) transport southwards towards the jet stream. Gill (1963) constructed idealized isentropic streamlines for the situation of the following two days (when the situation had not changed materially) and his results support the above model.

The inclusion of diabatic heating in the determination of vertical velocity would support this model. Kinetic energy generation ($\rho \bar{u} \bar{w}$) within the cloud zone would be increased as would the upward transport in this region.

For future consideration, more examples of a similar nature should be studied to confirm the suggested model. Also a study of available potential energy is necessary to complete the study of the energetics of the system. It may be that cross-equatorial transport of kinetic and available potential energy to the Indian Ocean is important. Here, in the upper troposphere, air which originates over the monsoon areas of Asia is transported across the equator into the southern hemisphere and may make an important contribution to the strength of the subtropical jet stream (Garreaud, 1975). The fact that this jet is more or less enhanced and the monsoon is weakened, strongly suggests that the monsoon does play a large part. The model suggested above may be, initially, a weak pole effect superimposed on the larger scale inter-hemispheric reaction. Thus an extension westward of the axis of incidence is indicated.

VIII. CONCLUSIONS

It seems that the tropical area, and in particular the cloud zone, may be a source of energy for the sub-tropical jet stream. Results from the previous section suggest a possible model of (i) kinetic energy generation within the cloud zone (ii) transport aloft to the upper troposphere, and then (iii) transport southwards towards the jet stream. Hill (1963) constructed isentropic streamlines for the situation on the following two days (when the situation had not changed materially) and his results support the above model.

The inclusion of diabatic heating in the determination of vertical velocity would support this model. Kinetic energy generation ($\omega \alpha'$) within the cloud zone would be increased as would the upward transport in this region.

For future consideration, more occasions of a similar nature should be studied to confirm the suggested model. Also a study of available potential energy is necessary to complete the study of the energetics of the system. It may be that cross-equatorial transport of kinetic and available potential energy in the Indian Ocean is important. Here, in the upper troposphere, air which originates over the monsoon areas of Asia is transported across the equator into the southern hemisphere and may make an important contribution to the strength of the subtropical jet stream (Ramage, 1970). The fact that this jet is more or less anchored and the monsoon is anchored, strongly suggests that the monsoon does play a large part. The model suggested above may be, relatively, a small scale effect superimposed on the larger scale inter-hemispheric reaction. Thus an extension westward of the area of interest is indicated.

Finally, the mesh size of the diagnostic model should be decreased by about one half, the number of levels increased, and friction and diabatic heating considered.

which provided computer time.

ACKNOWLEDGEMENT

Calculations were carried out on the I.E.M. 360/65 computer of the University of Hawaii Statistical and Computing Center which provided computer time.

- Vol. 96, No. 4, pp 215-226.
- Carpenter, J.F., 1968: "The Climatology of the Sub-tropical Jet Stream Associated with Rainfall over Western Australia", Australian Meteorological Magazine, Vol. 16, No. 3, pp 168-173.
- Charney, J.G., 1955: "A Note on Large scale Motions in the Tropics", Journal of Atmospheric Science, Vol. 12, No. 6, pp 607-609.
- Charney, J.G., and J. Eliassen, 1949: "A Fundamental Method for Predicting the Perturbations of the Middle Latitude Westerlies", Journal, Vol. 6, No. 2, pp 34-44.
- Hill, G.F., 1963: "The Weather in Lower Latitudes of the Southwest Pacific Associated with the Passage of Disturbances in the Middle Latitude Westerlies", Proceedings of the Symposium on Tropical Meteorology, Honolulu, New Zealand, Ed. J.K. Armitage, New Zealand Meteorological Service, pp 353-363.
- Holmes, S.D., 1963: "On the Dissipation of Kinetic Energy in the Atmosphere", Tellus, Vol. 15, No. 7, pp 26-32.
- Hoskins, B. and M. Washington, 1969: "On Global Initialization of the Primitive Equations. Part I", Journal of Applied Meteorology, Vol. 8, No. 5, pp 726-731.
- Krishnamurti, S.N., 1968: "A Diagnostic Balance Model for Studies of Weather Systems of Low and High Latitudes, Part II: Number Less than 1", Monthly Weather Review, Vol. 96, No. 4, pp 101-107.
- Kuo, S.C., 1966: "Kinetic Energy Generation and Dissipation in

REFERENCES

- Baumhefner, David, P., 1968: "Application of a Diagnostic Numerical Model to the Tropical Atmosphere", *Monthly Weather Review*, Vol. 96, No.4, pp 218-228.
- Campbell, A.P., 1968: "The Climatology of the Sub-tropical Jet Stream Associated with Rainfall over Eastern Australia", *Australian Meteorological Magazine*, Vol. 16, No.3, pp 100-113.
- Charney, J.C., 1963: "A Note of Large Scale Motions in the Tropics", *Journal of Atmospheric Science*, Vol. 20, No.6, pp 607-609.
- Charney, J.G., and A. Eliassen, 1949: "A Numerical Method for Predicting the Perturbations of the Middle Latitude Westerlies", *Tellus*, Vol. 1, No.2, pp 38-54.
- Hill, H.W., 1963: "The Weather in Lower Latitudes of the Southwest Pacific Associated with the Passage of Disturbances in the Middle Latitude Westerlies", *Proceedings of the Symposium on Tropical Meteorology*, Rotorua, New Zealand. Ed. J.W. Hutchings, New Zealand Meteorological Service, pp 353-363.
- Holopainen, E.O., 1963: "On the Dissipation of Kinetic Energy in the Atmosphere", *Tellus*, Vol.15, No.1, pp 26-32.
- Houghton, D. and W. Washington, 1969: "On Global Initialization of the Primitive Equations: Part I", *Journal of Applied Meteorology*, Vol. 8, No.5, pp 726-737.
- Krishnamurti, T.N., 1968: "A Diagnostic Balance Model for Studies of Weather Systems of Low and High Latitudes, Rossby Number Less than 1", *Monthly Weather Review*, Vol. 96, No.4, pp 197-207.
- Kung, E.C., 1966: "Kinetic Energy Generation and Dissipation in

- the Large Scale Atmospheric Circulations", *Monthly Weather Review*, Vol. 94, pp 67-82.
- Muffatti, A.H.J., 1963: "Aspects of the Tropical Jet Stream over Australia", *Proceedings of the Symposium on Tropical Meteorology*, Rotorua, New Zealand, Ed. J.W. Hutchings, New Zealand Meteorological Service, pp 72-88.
- Murakami, T., 1959: "The Energy Budget over the Far East during the Rainy Season", *Journal of the Meteorological Society of Japan*, Vol. 37, No.3, pp 83 -95.
- Murakami, T., 1970: "Initial Adjustment of Data in the Tropics", *Hawaii Institute of Geophysics, University of Hawaii*, pp 54.
- Palmer, C.E., 1952: "Tropical Meteorology," *Quarterly Journal of the Royal Meteorological Society*, Vo. 8, No.336, pp 126-164.
- Phillips, N.A., 1962: "Lectures on the Geostrophic Scale Theory", *Massachusetts Institute of Technology*.
- Ramage, C.S., 1960: "Notes on the Meteorology of the Tropical Pacific and Southeast Asia", *Geophysics Research Directorate*, Appendix 1.
- Ramage, C.S. 1970: "Meteorology of the South Pacific", *Symposium of the Scientific Exploration of the South Pacific*, National Academy of Sciences.
- Sadler, J.C., 1968: "Average Cloudiness in the Tropics from Satellite Observation", *Lecture Notes, Department of Geophysics University of Hawaii*.
- Smagorinsky, J., S. Manabe, and J. Leith Holloway, Jnr., 1965: "Numerical Results from a Nine-Level General Circulation Model of the Atmosphere", *Monthly Weather Review*, Vol. 93,

No.12, pp 727-768.

Trout, D., and H.A. Panofsky, 1969: "Energy Dissipation Near
the Tropopause", *Tellus*, Vol. 21, No.3, pp 355-358.